World Academy of Science, Engineering and Technology
International Journal of Physical and Mathematical Sciences
Vol:5, No:2, 2011

Surface Plasmon Polariton Excitation by a Phase Shift Grating

T. Nakada, Y. Nakagawa, M. Haraguchi, T. Okamotoi, M. Flockert, T. Isu, G. Shinomiya

***Abstract*—** We focus on the excitation and propagation properties of surface plasmon polariton (SPP). We have developed a SPP excitation device in combination with a grating structures fabricated by using the scanning probe lithography. Perturbation approach was used to investigate the coupling properties of SPP with a spatial harmonic wave supported by a metallic grating. A phase shift grating SPP coupler has been fabricated and the optical property was evaluated by the Fraunhofer diffraction formula. We have been experimentally confirmed the induced stop band by diffraction measurement. We have also observed the wavenumber shift of the resonance condition of SPP owing to effect of a phase shift.

***Keywords*—**Surface Plasmon Polariton, phase shift grating, scanning probe lithography

I. Introduction

THE Surface Plasmon Polariton (SPP) is a coupling of a plasma wave with an electromagnetic wave at the surface as it is well known [1]. In last decade, many sensing applications have been developed employing SPP. Moreover, the development of fabrication and observation technologies for nano-sized structures benefits the research activities of SPP. One of the useful tools for nano-scale sciences and technologies is a scanning probe microscope (SPM). When we employ the SPM for the lithography, the probe of SPM works as a patterning tool for nano structure developed in 1990th [2]. We have demonstrated previously, that SPM is a powerful fabrication and observation tool for SPP devices [3]. The grating structure was drawn on the surface of a conductive Si substrate surface by probe anodization lithography. Post chemical etching and other processes were applied to fabricate the SPP grating coupler and the wave guides. In this paper, the trial fabrication of SPP devices with integrated slab waveguide was accomplished by using the SPM lithography. Optical diffraction measurement was performed to demonstrate the function of the fabricated grating as a SPP coupler.

T. Nakada is with Department of Optical science and technologies, The University of Tokushima, Minamijosanima 2-1, Tokushima 7708506 Japan (corresponding author to provide phone: +81-88-656-9411; fax: +81-88-656-9411; e-mail: nakada@opt.tokushima-u.ac.jp).

Y. Nakagawa is with Center for Frontier Research of Engineering, The University of Tokushima, Minamijosanima 2-1, Tokushima 7708506 Japan (e-mail: yosinori@frc.tokushima-u.ac.jp). He is also with Nichia Corporation, Oka 491 Kaminaka Anan Tokushima 7748601, Japan

M. Haraguchi is with Department of Optical science and technologies, The University of Tokushima, Minamijosanima 2-1, Tokushima 7708506 Japan (e-mail: haraguti@opt.tokushima-u.ac.jp).

T. Okamoto is with Department of Optical science and technologies, The University of Tokushima, Minamijosanima 2-1, Tokushima 7708506 Japan (e-mail: okamoto@opt.tokushima-u.ac.jp).

M. Flockert is with Department of Optical science and technologies, The University of Tokushima, Minamijosanima 2-1, Tokushima 7708506 Japan (e-mail: flockert@opt.tokushima-u.ac.jp).

T. Isu is with Center for Frontier Research of Engineering, The University of Tokushima, Minamijosanima 2-1, Tokushima 7708506 Japan (e-mail: t.isu@frc.tokushima-u.ac.jp).

G. Shinomiya is with Nichia Corporation, Oka 491 Kaminaka Anan Tokushima 7748601, Japan (e-mail: genichi.shinomiya@nichia.co.jp)

A part of this research was supported by KAKENHI 21310082.

II. Theoretical

A. The Fraunhofer diffraction of the optical grating

In general, the optical diffraction by grating structures in the far field is described by the Fraunhofer diffraction formula as it is well known [4]. We employed the formula for the optical multi slit to estimate the properties of the grating structure with the grating parameters, i.e. lattice constant d, duty and amplitude, which are dominant factors to affect the SPP excitation properties. As for a plain grating with d, the diffraction angular distribution is described by the following formulas for the incident plane wave with a wavelength λ in vacuum,

$$I = I_o(\sin(\phi)/\phi)^2(\sin(N\varphi)/\sin\varphi)^2 \quad (1a)$$

$$\phi = (\pi/\lambda)a(\sin(i_0)+\sin(i_1)) \quad (1b)$$

$$\varphi = (\pi/\lambda)d(\sin(i_0)+\sin(i_1)) = (d/a)\phi \quad (1c)$$

where i_o; incident angle, i_1; diffraction angle, I_o; incident beam intensity, a; aperture size of grating, N is the grating slit numbers which contribute the optical diffraction, respectively. We neglect the contribution from the groove region of the grating. For the phase shift grating, the phase retardation was considered in same procedure to obtain the theoretical description of the angular diffraction pattern.

B. A modified 1st order perturbation treatment of SPP excitation by a grating structure

The grating causes the spatial harmonic waves of the incident optical plane wave to couple with the SPP wave at the crossing pints of the dispersion relations in Bllirouin diagram [5]. Here, this phenomenon was treated with modified first order perturbation theory proposed by Yamashita and Tsuji [6]. Figure 1, shows the case of the p-polarized incident optical wave is in the x-z plane. The interface between air and the metallic film has a sinusoidal shape with an amplitude h and a period d; it can be described as,

$$Z = \xi(x) = \xi_{+g}\exp(jg_x) + \xi_{-g}\exp(-jg_x) \quad (2)$$

, where g=2π/d and h=2|ξ g |. The amplitude of the grating is assumed to be enough smaller than λ, and d.

The resonant coupling excitation of SPP mode, i.e., the excitation of SPP, can be monitored by the dips in the angular spectrum of the reflection, i.e., 0th order diffraction, intensity. In Fig. 1, the magnetic field amplitudes of incident, reflected and penetrated waves are denoted as B_i, B_r and B_t, respectively. These waves has the same x-component of a wave number; $k_x=(2\pi/\lambda)\sin(\theta_o)$. In this paper, the two wave approximation was used. Namely, we just considered the wave coupling between +1st order diffracted optical wave and SPP wave near the phase match condition. The other spatial harmonics contribution is ignored. The coupling wave has the wave number; $Kg=k_x+g$. We denote the amplitude of the coupled wave as B_g, on the air side and B_{gt} on the metallic side. From the boundary condition for B at the surface, we can obtain the liner simultaneous equations for B_r, B_t, B_g and B_{gt} if B_i is given.

$$\frac{B_r}{B_i} = \begin{vmatrix} -(k_z\varepsilon - i\gamma) - |\xi_g|^2(k_z\eta + i\gamma\xi\varepsilon) & i\xi_{-g}(1-\varepsilon)(k_yK_g - \gamma\Gamma_g) \\ -i\xi_g(1-\varepsilon)(k_yK_g - ik_z\gamma_g) & -i(\Gamma_g\varepsilon + \gamma_g) - i|\xi_g|^2(\Gamma_g\eta + \gamma_g\xi\varepsilon) \end{vmatrix} \Big/ \begin{vmatrix} -(k_z\varepsilon - i\gamma) - |\xi_g|^2(k_z\eta + i\gamma\xi\varepsilon) & i\xi_{-g}(1-\varepsilon)(k_yK_g - \gamma\Gamma_g) \\ i\xi_g(1-\varepsilon)(k_yK_g + ik_z\gamma_g) & -i(\Gamma_g\varepsilon + \gamma_g) - i|\xi_g|^2(\Gamma_g\eta + \gamma_g\xi\varepsilon) \end{vmatrix} \quad (3)$$

The reflection coefficient is shown as eq.3 and the energy reflectivity is given by $|Er|^2/|Ei|^2=|Br|^2/|Bi|^2$. Where, $K_g=K_y+g$, $K_y^2+K_z^2=(2\pi/\lambda)^2$, $K_g^2-\Gamma_g^2=(2\pi/\lambda)^2$, $k_y^2-\gamma^2=(2\pi/\lambda)^2\varepsilon(\omega)$, $K_g^2-\gamma_g^2=(2\pi/\lambda)^2\varepsilon(\omega)$, $\xi=(2\pi/\lambda)^2-k_yK_g$, $\eta=(2\pi/\lambda)^2\varepsilon(\omega)-k_yK_g$, c; light speed in vacuum, respectively. The factor of $|E_g/E_i|^2=(1+2\Gamma_g^2/(2\pi/\lambda)^2)|B_g/B_i|^2$ shows the field enhancement factor.

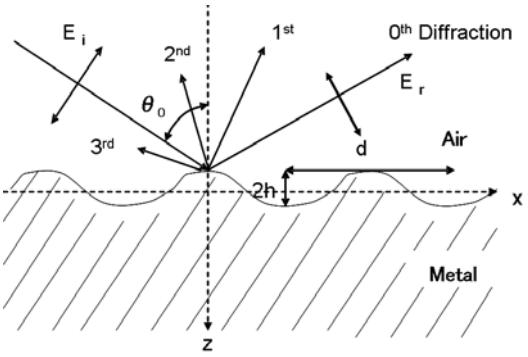

Fig.1 Schematic representation of a metallic grating and notations

The p-polarized in the x-z plane is focused on a metallic film from the air with an angle of incidence θ_0. The interface between air and the metallic film has a sinusoidal shape with an amplitude h and period d.

III. Experimental

A. The SPM lithography and a grating fabrication

The surface anodization process by scanning probe microscope (SPM) is controlled by the lateral scanning speed of probe and the applied voltage between the probe and surface of the sample, mainly, under atmospheric conditions. The applied voltage is normally changed from 0 to 50V DC depending the material and line width. The probe scanning speed is changed between 0.01 to 1000μm/s. High speed anodization lithography can be successfully achieved with a speed of 1mm/s on conductive Si surfaces. It is very helpful to draw the large size grating patterns.

A post chemical etching in 25 wt% KOH solutions at a suitable temperature is performed to get the grating structure by using the anodized pattern as a mask. The ratio between Si and SiO_2 etching rates is approximately 100. With a few nm thick anodized masking layer, it is possible to fabricate Si surface structures with several 100nm depth.

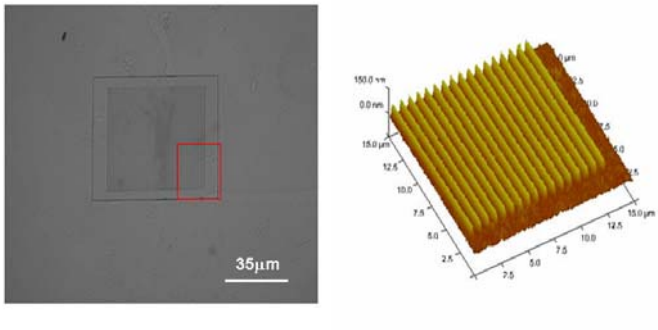

(a) (b)

Fig. 2 Optical (a) and AFM topographic (b) images of a grating fabricated by SPM lithography and post etching

We show a typical grating structure fabricated by the SPM lithography and the post etching in Fig.2. As shown in Fig.2 (a),

a grating structure with a period of 1.15μm and an amplitude of 50nm was fabricated over an area of 70μm × 70μm.

Following the etching, an oxidation layer was grown at the Si surface by dry thermal oxidation process. The oxidation layer works as an isolating layer to prevent the penetrating of SPP field into the high refractive index material; Note that Si for visible light that would cause a high damping. The Au or Ag film with 50nm thickness was evaporated on the oxidized layer at the sample surface by RF-spattering. The cross section view taken by scanning transmission electron microscope (STEM) of the fabricated SPP grating coupler is shown in Fig. 3. The thicknesses of the SiO_2 and Au layers are 150nm, 50nm respectively. The grating amplitude is 50nm.

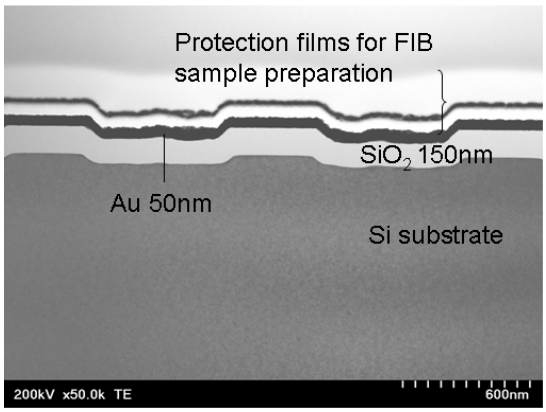

Fig. 3 STEM image of the cross section of the SPP grating coupler

B. Optical and SPM investigation of the grating

The Fraunhofer diffraction pattern of the fabricated grating coupler was measured by angle scan method. A TM polarized He-Ne laser beam (632.8nm 1mW), was focused on the grating area by a lens with f=20mm. The spot size is approximately 20 to 50μm in diameter. The sample was placed at the rotation center of a goniometer stage. The reflected and the diffracted lights were detected by a Si pin photodiode detector. For the measurement, the position of the detector was scanned to detect diffracted light in the angle range from -20° to 80°. The angle of incident was fixed at 45° or 60°, through the diffracted angle. The angular resolution of the diffracted light intensity was in range from 0.1° to 0.5° which was limited the width of a mechanical slit in front of the photo diode. The observed diffracted light intensity distribution for the plain grating, single phase shift grating and 45° blazed gratings are shown in Fig. 4 (a), 4 (b) and 4 (c), respectively.

In order to evaluate the grating, we calculated the theoretical angular diffraction spectra. The fraunhofer formulas were modified taking into account the phase retardation at the phase and at the angular shifts for the phase shift and the blazed gratings, respectively. In Figs. 4, we show the theoretical spectra fitted to the experimental ones as the dashed lines. The theoretical curves agree well with the experimental ones.

In Fig. 4 (b), a sharp dip in the diffraction spectra peak at around 8°, i.e. 1st order diffraction peak, is observed. The phase shift grating can modify the SPP excitation condition depending on the value of the phase shift. The value matched to form a stop band on the 1st order diffraction peak.

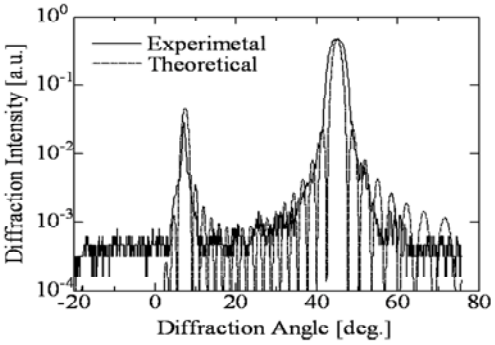

(a)

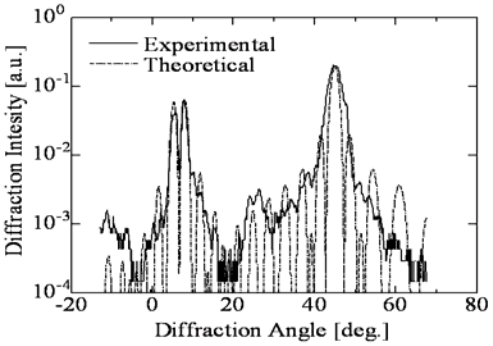

(b)

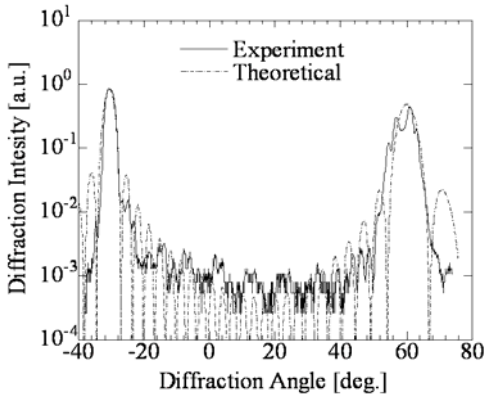

(c)

Fig. 4 Diffraction light intensity spectra, i.e., angular diffraction spectra of (a) plain grating, (b) a phase shift grating and (c) a blazed grating. Blazing angle is approximately 45°.

A blazed grating can generate strong spatial harmonic waves. We, therefore, designed the blazed grating to generate such the waves at the phase-matched angle of SPP in order to bring higher coupling effiency between SPP and the incident beam than that for the plane grating. In Fig. 4 (c), the blazed effect is obviously observed as the fact that the peak intensity at around -30°, i.e., the 1st order diffraction intensity, is stronger than that reflection spot at 60°, i.e., the 0th order diffraction intensity.

Note that the 1st order diffraction intensity is lower than the 0th order diffraction intensity in Fig. 4 (a) and (b).

C. SPP excitation by angular scanning

We measured the reflection intensity of the 0th diffraction varying with the angle of incidence, i.e., angular scanned reflection intensity, to confirm a SPP excitation. The TM-polarized He-Ne (632.8nm) and LD (680nm) light sources were used for the excitation and a Si pin photo diode was used to detect the reflected light intensity.

Figure 5 (a) shows the angular reflection spectra of the plane grating where the solid line and dots are for the He-Ne and for the LD light sources. The dips of the reflection intensity at 25° for the dots and 30° for the solid line correspond to the SPP excitation. Considering a grating constant of 1.15μm and the dispersion relation of the dielectric constant Au, these angles of the dips agree with those expected as those for the SPP excitation.

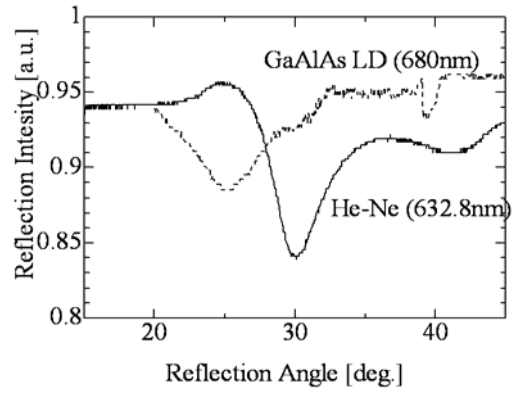

(a)

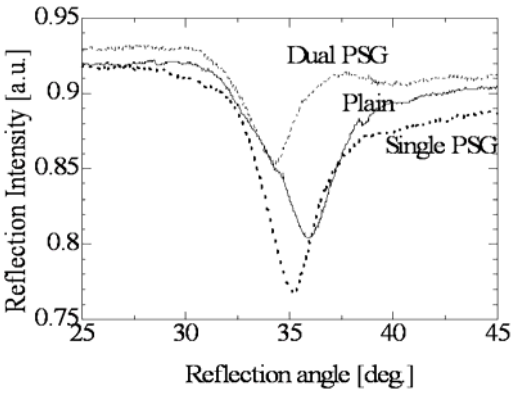

(b)

Fig. 5 SPP excitation by angular scanning (a) for plain grating, for Au film (b) for phase shift gratings with Ag film.

As for the phase shift grating, we make same measurement with He-Ne laser (632.8nm). The data is shown in Fig. 5(b), the solid line, dots and the dashed line are for plain, single phase shift grating and double phase shift grating. The resonance excitation angle of SPP shifts to the lower wave number by the stop band creation.

IV. Results and Discussions

A. The optical diffraction measurement results

We have evaluated the grating lattice parameters from the AFM and optical measurement results. The former were obtained from analyzing the topographic images of the gratings. The latter was obtained by analyzing the diffracted light intensity spectra in Figs. 4 with the Fraunhofer diffraction formula. In table 1, we show the evaluated parameters for the grating. The parameters by the former and the latter agree well with each other. This implies that Fraunfoher diffraction formula of the multi slits case is suitable for analyzing the optical characteristics of a grating device with similar structure to those of our sample. The side robe suppression in the diffracted light intensity spectra comes from an appodization effect by a Gaussian beam intensity profile of He-Ne TEM_{00} mode laser employed here.

Table I Grating Parameters Estimated By AFM And Optical Measurement Results

Item	Diffraction			AFM		
Sample	A	B	C	A	B	C
Lattice c. [um]	1.42	1.09	0.93	1.42	1.10	0.93
Slit width [um]	1.12	0.81	0.61	1.07	0.84	0.58
depth [nm]	-	-	-	130	120	180

B. SPP excitation experiment results

Figure 6 (a) and (b) show the theoretical reflection intensity depending on the angle of incidence and the angle of diffraction for a Au plain gratin, respectively. The former displayed the variation of the reflection intensity with the excitation wavelength λ for the grating with a lattice constant d of 1.15 μm. The latter displayed the variation of the reflection with d for the λ = 632.8nm. The angles of dip in Fig. 6 (a) for λ = 632.8nm and 680nm agree with the experimental resonance dips in Fig. 5 (a).

Figure 7 shows the comparison between the theoretical angular reflection spectra for varies grating depth and experimental angular reflection spectrum for a Au grating with a grating depth of 70nm at λ = 632.8nm. For the calculation, d was set to be 1.06μm. Compared with theoretical spectra, the dip of the experimental one at 32° is much shallow and wide. This may come from the imperfection of the grating structure and the dielectric loss contributed by the Si substrate.

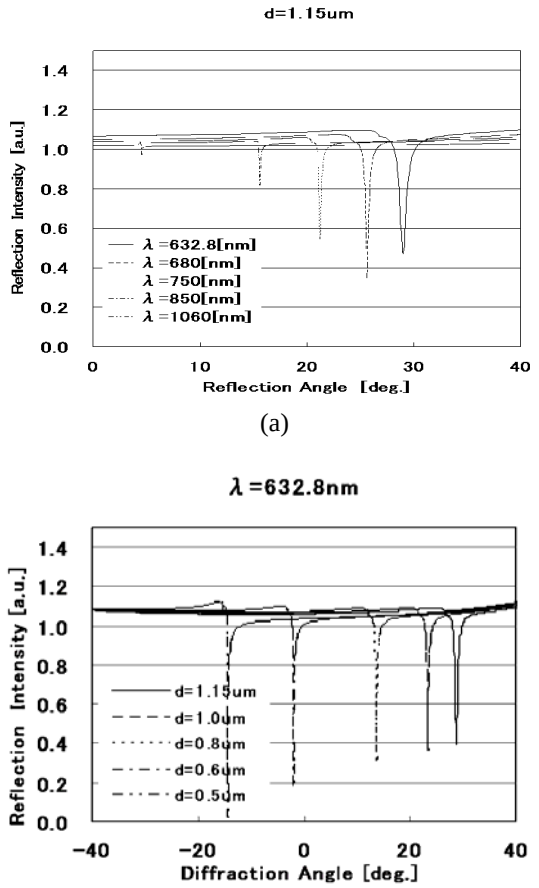

Fig. 6 Theoretical investigation of angular reflection spectra for SPP grating coupler with Au film, (a) for wavelength dependence and (b) for grating constant dependence.

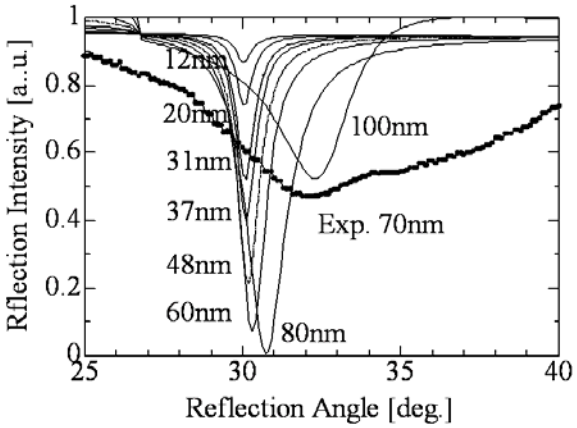

Fig. 7 Grating depth dependence of the angular reflection spectra around SPP excitation angle

V. Conclusion

A several types of grating SPP couplers was successfully fabricated by the SPM lithography and post treatments on a metal surface on top of a conductive Si substrate. Especially a blazed grating coupler was fabricated that showed a ten times enhancement of the diffraction intensity compared to that by a non blazed grating for the $+1^{st}$ order. We have also observed SPP mode excitations in our gratings using an angular scanned spectra configuration. The coupling of the spatial harmonic wave by the multi-phase shift grating modified the dispersion relation of SPP and induced the shift of the excitation angle for SPP.

As future prospects, SPP coupling devices will be fabricated with slab SPP waveguides in order to control their propagation properties and build functional plasmon devices by using SPM lithograph and the post treatment in this report.

Acknowledgment

We are grateful to Mr. Okazaki in Nichia Corporation for his STEM observation and FIB treatments. A part of this research was supported by KAKENHI 21310082.

References

[1] V.M.Agranvich and D.L.Mills, “Surface Polaritons”, New York, North-Holland Publishing Company, 1982, p93.
[2] P.Avoulis, T.Heltel and R.Martel,"Atomic force microscope tip-induced local oxidation of silicon: kinetics, mechanism, and nanofabrication” Appl. Phys. Lett. 71 (1997) pp.285-287.
[3] T. Nakada, M. Haraguchi, Y. Nakagawa, M. Fukui, T. Okamoto, T. Isu and G. Shinomiya, “Fabrication of a grating coupler in Surface Plasmon Polariton (SPP) waveguide by Scanning Probe Microscope (SPM) lithography”, Technical Digest of the 7th Asia-Pacific Conference on Near-Field Optics, Jeju, 2009, p70.
[4] A. Sommerfeld: OPTIK 3rd edition (1965).
[5] B.Fischer, N.Marschall, and H.J.Queisser: Surface Sci., 34 (1973) 50.
[6] M Yamashita, M Tsuji,”Simple Theory for Surface-Plasmon-Polariton Resonance on Sinusoidal Metal Surface:Application to SERS” J. Phys. Soc. Jpn., 52 (1983) pp.2462-2471.